Zeolite Types Used in Catalytic Methane Combustion

Subjects: Environmental Sciences

Contributor: Jinxiong Tao, Yuxi Liu, Jiguang Deng, Lin Jing, Zhiquan Hou, Lu Wei, Zhiwei Wang, Hongxing Dai

The emission of methane leads to the increase in the methane concentration in the atmosphere, which not only wastes resources but also intensifies the greenhouse effect and brings about serious environmental problems. Catalytic combustion can completely convert methane into carbon dioxide and water at low temperatures. However, the catalytic activities of the conventional supported palladium catalysts (e.g., Pd/Al_2O_3 and Pd/ZrO_2) are easy to decrease or the two catalysts can even be deactivated under actual harsh reaction conditions (high temperatures, steam- and sulfur dioxide-containing atmospheres, etc.). Noble metal catalysts supported on zeolites with ordered pores and good thermal stability have attracted much attention.

Keywords: methane combustion ; zeolite ; supported noble metal catalyst ; palladium-based catalyst

1. Introduction

As an attractive energy source, methane is more economical and friendly to the atmosphere than the other fossil fuels, and furthermore, methane possesses a high energy density with a high H/C ratio. Natural gas (its main component is methane) can be used as a fuel in compressed natural gas (CNG) vehicles, and its combustion in CNG vehicles leads to lower emissions of CO_2, CO, non-CH_4 hydrocarbons, and NOx than that in traditional diesel or gasoline vehicles. It has been reported that the above emissions could be significantly reduced if the energy source was replaced by natural gas [1][2]. With a higher fuel combustion efficiency, lean-burn natural gas vehicles (NGVs) emit up to 21% less greenhouse gas than their gasoline or diesel counterparts. Complete oxidation of methane to CO_2 can effectively reduce its environmental impact by more than 96% as compared with the direct emission of methane to the atmosphere. Up to now, it has been well-recognized that CH_4 plays an indispensable role in the paradigm shift to a more sustainable planet. However, natural gas engines still emit significant amounts of unburnt CH_4 (so-called methane slip) in stationary applications (power plants). The lifetime of CH_4 in the atmosphere is much shorter than CO_2, but CH_4 is more efficient than CO_2 in trapping radiation. In the past 100 years, the global warming potential of CH_4 has been reported to be 28–36 times higher than that of CO_2 [3][4][5].

Catalytic combustion of CH_4 provides an alternative pathway to its thermal combustion. Under the fuel-lean conditions, due to the overheating of methane combustion, more nitrogen oxides are produced. Due to the high temperatures generated during the methane combustion process under the fuel-lean conditions, more nitrogen oxides are produced. For the combustion of low-concentration methane, the emergence of adsorption enrichment technology provides another pathway for the comprehensive utilization of lean methane. Membrane separation and pressure swing adsorption technologies are mainly used in practice, which can enrich the methane concentration. However, it is not widely used in industry because the costs of operation and preparation exceed the economic benefit of increasing the concentration. An ideal catalyst design should take into consideration the low-temperature operation and long-term stability [6]. The low operation temperature is important in minimizing the generation of the secondary pollutants emissions (e.g., NO_x) in CH_4 combustion or making the system achieve low CH_4 emission standards for the removal of CH_4.

Up to now, there have been a large number of catalysts (transition metal oxides, mixed metal oxides (e.g., ABO_3, A_2BO_4, and $A_2B_2O_7$), (conventional supports or zeolites)-supported noble metals, and hexaaluminates ($MAl_{12}O_{19}$)) developed in the literature. The noble metal-based catalysts used in methane combustion are mainly Pd, Pt, Rh, and Au. Generally speaking, their activity sequence is Pd > Pt > Rh > Au. Among them, Rh is expensive and easy to volatilize and lose at high temperatures, while Au has the worst activity for methane combustion and is generally used as a cocatalyst, such as Pd-Au, Pt-Au, etc. Pd shows the highest activity and light-off activity at low temperatures, and it is not volatile at high temperatures. Moreover, Pd-based catalysts exhibit better catalytic performance for the combustion of alkanes (C_{3+}). In addition, some non-Pd-based catalysts are discussed later. Compared with the other noble metal catalysts, supported Pd catalysts are the most widely and deeply studied. Although the microscopic mechanism is still unclear, we can get a glimpse of catalytic methane combustion with the development of more advanced characterization methods and

theoretical computational chemistry. Up to now, various catalysts have been developed to promote CH_4 combustion, including platinum group metals (PGM), transition metal (no-PGM) oxides, perovskite-type or -like oxides, and hexaaluminates [7][8][9][10][11][12][13]. To date, there have been some review articles on catalytic CH_4 combustion in the literature [3][7][14], which summarized the catalyst choice and their properties, support effects, active center nature, reaction kinetics, water resistance, and sulfur dioxide-poisoning mechanism, as well as the impact of the operating conditions. Among all the reported catalysts, platinum group catalysts show the highest intrinsic activities at low temperatures and can achieve a nearly 100% CH_4 conversion below 600 °C. However, the reaction rates of transition metal oxide catalysts are generally lower by 3–5 orders of magnitude, and methane conversion can reach 100% only at an operating temperature above 600 °C.

In the past decades, there has been a tremendous interest in developing high-performance low-temperature CH_4 oxidation catalysts [15][16], and the Al_2O_3-supported Pd-based materials remain one of the highly efficient catalysts. Of course, Pt- and Rh-based catalysts are also considered to be excellent candidates for catalytic methane combustion. Although Pt is typically doped in commercial catalysts to improve the thermal stability and sulfur dioxide resistance, Pd is the major catalytic active site. The big challenge is that H_2O (typical concentration = 5–15 vol%) and SO_2 (typical concentration = 1–30 ppm) in the exhaust gas results in severe deactivation of the catalysts that decrease the CH_4 removal efficiency. Many available supports have been reported, such as Al_2O_3 [17][18][19][20][21][22][23], CeO_2 [24][25][26][27], $Ce_{1-x}Zr_xO_2$ solid solutions [28][29][30], and SnO_2 [31][32][33][34]. Zeolites with various additives have also been used in methane combustion. Each type of support possesses some beneficial features. For instance, Al_2O_3 has a relatively low cost and a large specific surface area. CeO_2- and $Ce_{1-x}Zr_xO_2$-supported catalysts exhibit a large oxygen storage—release capacity due to the presence of the Ce^{4+}/Ce^{3+} redox couple, while doping Zr into the lattice of CeO_2 to form a Ce-Zr solid solution can strongly improve the thermal stability of the catalyst. Zeolite-supported catalysts demonstrate better water tolerance than other compounds-supported catalysts. Of course, each of these catalysts possesses some obvious advantages and disadvantages. The noble metal components are generally supported on various metal oxides (e.g., Al_2O_3, CeO_2, ZrO_2, Co_3O_4, and SiO_2) for lean methane combustion. For example, the Pd/CeO_2 and $Pd/Ce_xZr_{1-x}O_2$ catalysts exhibited a better performance at low temperatures than other supported noble metal catalysts due to the support of CeO_2 or $CexZr_{1-x}O_2$ possessing the Ce^{4+}/Ce^{3+} redox couple that could indirectly affect the performance of the catalyst, while doping Zr to the lattice of CeO_2 to generate a Ce-Zr-O solid solution could strongly improve the thermal stability of the catalyst [28][29]. Willis et al. [35] used SiO_2 (inert), Al_2O_3 (acidic), $Ce_{0.8}Zr_{0.2}O_2$ (redox), and MgO (alkaline) as support materials and found that, although the above oxide-supported Pd catalysts possessed similar activation energies for methane combustion, the activity of the MgO-supported Pd catalyst was obviously low. The authors believed that basic MgO enhanced the stability of the electron-rich PdO phase, which led to the increase in energy required to form oxygen vacancies and the decrease in the methane reaction rate. In addition, MgO could easily adsorb CO_2 to generate magnesium carbonate, which covered the active sites, influencing the surface of the Pd particles or the interface between the Pd and the carrier, and hence giving rise to a decreased catalytic activity.

It is well-known that low-temperature CH_4 oxidation over Pd-based catalysts follows a Mars—van Krevelen (MvK) redox mechanism. Garbowski et al. investigated the physicochemical properties of the Pd/*γ*-Al_2O_3 catalyst by combining nano-diffraction, electron microscopy, and Fourier transform IR (FT-IR) analysis [36]. The authors proved that the MvK reaction mechanism was suitable for explaining the kinetic behavior of CH_4 oxidation. Over the supported noble metal (e.g., Pd and Pt) catalysts, CH_4 is first adsorbed on the surface of the active nanoparticles (NPs) and dissociated into the adsorbed methyl species. Because methane has a highly symmetrical tetrahedral structure with a C–H binding energy of 435 kJ/mol, the first step of bond breaking is the rate-limiting step [37]. Under the action of oxygen, intermediate species (such as HCHO and carbonate) are generated and finally converted to CO_2 and H_2O as products. The catalytic activity of methane oxidation is controlled by different oxygen species, among which lattice oxygen (O_{latt}) and surface oxygen (O_{sur}) are the main oxygen species. In the low-temperature stage of CH_4 oxidation, the increase in the amount of the O_{sur} species can greatly enhance the catalytic activity of the catalyst, while in the high-temperature stage of CH_4 oxidation, the increase in the amount of the O_{latt} species can greatly improve the catalytic activity of the catalyst. In this process, the adsorption and desorption between CH_4 and CH_4^* are very fast processes, and at the same time, the gas-phase oxygen in this process combines with the catalyst to generate a series of O_{sur} and O_{latt} species, so the rapid transformation of CH_4^* and [O] is a critical factor in the catalytic combustion of low-concentration CH_4.

As pointed out above, Pd-based catalysts are thought to be the most active for combustion of CH_4 under lean conditions. It is known that the activity of the Pd/Al_2O_3 catalyst is seriously inhibited by water vapor and its gradual deactivation takes place. Promotion brought about by suitable supports has been reported. A support is important for enhancing the catalytic activity and stability of a supported noble metal catalyst. In comparison to *γ*-Al_2O_3, *α*- and *θ*-Al_2O_3 could offer weaker Pd-Al_2O_3 interactions that helped to expose more Pd step sites [38]. Upon increasing the calcination temperature, the crystalline structure of ZrO_2 was transformed from the mixed phase (monoclinic and tetragonal) to the pure tetragonal

phase, and the tetragonal ZrO_2-supported Pd catalysts exhibited good hydrothermal stability [39]. Moreover, doping part of the Zr to the lattice of CeO_2 to form a $Ce_{1-x}Zr_xO_2$ solid solution can greatly improve the thermal stability of the $Ce_{1-x}Zr_xO_2$-supported noble metal catalyst. Although such a deactivation is reversible to some extent, it affects the normal working status of the catalyst in a specific environment. Schwartz et al. thought that H_2O poisoning of the supported Pd catalyst was caused by the adsorbed OH species, which covered the catalyst surface to form the stable and inactive $Pd(OH)_2$ phase [40]. However, the intrinsic CH_4 combustion activity of Pd/SiO_2 is much lower than that of Pd/Al_2O_3. Different from Pd/SiO_2, Pd/Al_2O_3 experienced severe low-temperature steam poisoning when it was exposed to an excessive steam atmosphere. As a unique class of microporous and crystalline solids, aluminosilicate zeolites have hence been considered to be one possible selection for decreasing the negative effect of water on CH_4 combustion. Aluminum oxide and zirconium oxide are usually used as supports for loading the noble metals in methane combustion. In addition to aluminum oxide and zirconium oxide, zeolites are also a kind of important support used for loading the noble metals.

Zeolites are an attractive class of shape-selective materials with regular microporous aluminosilicates, controlled acidity, and good (hydro)thermal stability. Such microporous materials have been used in adsorption and separation, petroleum refining, energy and chemical industries, environmental protection, and other fields because of their structural characteristics (pore structures and pore sizes), specific adsorption performance of small molecules, and high specific surface areas [41]. The framework illustrations of the support types of the main zeolites and some mesoporous silicas were used for the complete combustion of methane here, as shown in **Table 1** and **Figure 1**. Zeolites are also effective catalytic materials, although they cannot catalyze methane combustion independently. For this reason, zeolites are often used as supports for dispersing metal NPs to increase functionality. Complex strategies are also developed to prepare composite zeolites with core-shell structures. Specifically, the design and development of zeolite-supported metal catalysts (e.g., precious metals) and NPs doped in zeolites have strengthened the application of zeolites in CH_4 activation.

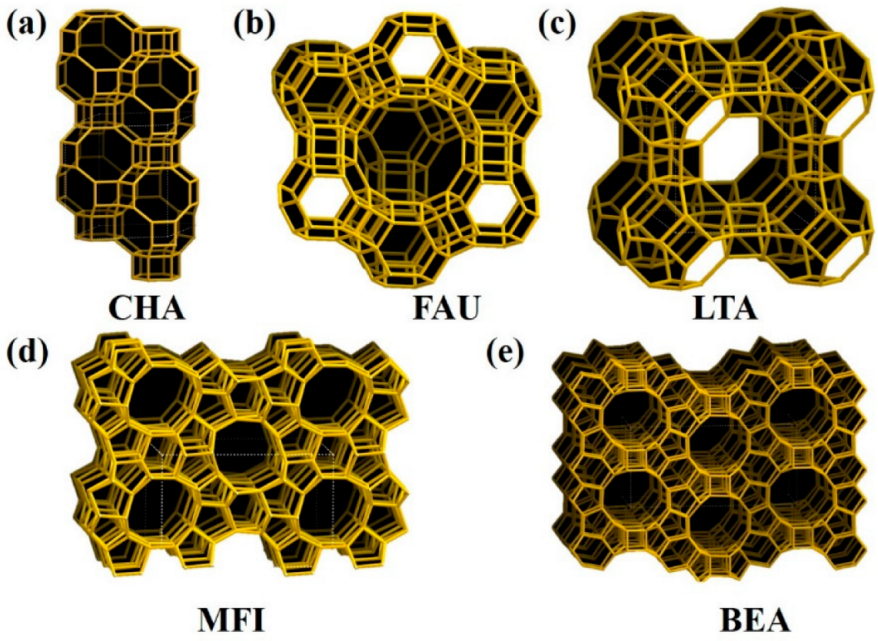

Figure 1. Framework images of (**a**) CHA, (**b**) FAU, (**c**) LTA, (**d**) MFI, and (**e**) BEA (obtained from the IZA-SC).

Table 1. Structural properties of zeolites with different topologies and mesoporous silicas.

Framework Type	Material Name	Dimensionality	Ring Type (Pore Type)	Limiting Pore Size (nm)
CHA	SSZ-13	3D	8/6/4 (micropore)	0.38 × 0.38
LTA	LTA	3D	8/6/4 (micropore)	0.41 × 0.41
MFI	ZSM-5	3D	10/6/5/4 (micropore)	0.53 × 0.56
BEA	Beta	3D	12/6/5/4 (micropore)	0.66 × 0.67

Framework Type	Material Name	Dimensionality	Ring Type (Pore Type)	Limiting Pore Size (nm)
FAU	X, Y	3D	12/6/4 (micropore)	0.33 × 0.33
SBA-15	-	1D	-/-/- (mesopore)	4.6–10.0 [42]
MCM-41	-	1D	-/-/- (mesopore)	10.0 [43]
KIT-6	-	3D	-/-/- (mesopore)	4.0–12.0 [44]

Note: The information for the microporous zeolites is obtained from the “Database of zeolite structures” by the Structure Commission of the International Zeolite Association (IZA-SC), whereas the information for the mesoporous zeolites is cited from the references as noted.

2. Small-Pore Zeolites with 8 Member Rings

SSZ-13 is a typical CHA-structured molecular sieve with small pores and eight member rings, which has a large specific surface area and an abundant acid amount. Zeolites with eight member rings have a high potential to inhibit the aggregation of metal cations under reaction conditions due to their small pore sizes (0.38 nm × 0.38 nm) and good hydrothermal stability compared with the medium- and large-pore zeolites. Recently, Cui et al. have reported that when the Pd loading in Pd/SZZ-13 was increased to 2 wt% or more, the sizes of the PdO particles were 2.5 ± 1.5 nm; the decrease in the CH4 oxidation rate with the drop in Pd content was attributed to the generation of a greater amount of the isolated Pd(II) ions that were less active than the PdO NPs formed at higher Pd contents [45]. These findings are in good agreement with those previously reported by Friberg et al. [46]. However, the hydrothermal aging of SSZ-13 at high temperatures (>850 °C) can cause structural destruction, giving rise to a decreased surface area, pore volume, and change in the XRD pattern [47]. Friberg et al. studied the effect of Pd loading on CH_4 oxidation of the thermally stable LTA zeolite with a Si/Al ratio of 44 and after hydrothermal aging at temperatures as high as 900 °C [48]. After hydrothermal aging at temperatures of ≤700 °C, the Pd/LTA exhibited a high and stable CH_4 combustion performance in the presence of water vapor. These authors found that the deactivation of the catalyst was not caused by the structural collapse of the LTA zeolite, and the $T_{50\%}$ over the Pd/LTA was 41 °C lower than that over the Pd/Al_2O_3. After thermal aging at 700 °C, the difference in the $T_{50\%}$ was 20 °C. Thermal aging at higher temperatures (800 and 900 °C) resulted in a higher $T_{50\%}$ (68 and 118 °C) over the Pd/LTA, respectively.

3. Medium-Pore Zeolites with 10 Member Rings

ZSM-5 was first synthesized in 1972 using the hydrothermal method with quaternary ammonium salts as the template agent [49]. The pore size of ZSM-5 is 0.55 nm × 0.51 nm, and this material shows a 10-element ring pore with a linear shape parallel to the *b*-axis direction and an elliptical pore with a pore size of 0.53 nm × 0.56 nm. As early as 1994, Li and Armor loaded Pd on ZSM-5 through the ion exchange approach and found that Pd/ZSM-5 exhibited excellent low-temperature methane combustion activity [50]. The higher catalytic activity of the Pd-based zeolite catalyst has been thought to be related to the additional lattice oxygen that can readily activate methane at low temperatures. All the zeolite catalysts reported in these early studies were prepared by the ion exchange method. Liu et al. pointed out that the glow discharge plasma treatment of the Pd-loaded zeolite catalysts before calcination could reduce the light-off temperature and improve the stability of the catalysts [51]. Hosseiniamoli et al. evaluated the stability of Pd/TS-1 and Pd/Silicalite-1 at 400 °C and a relative humidity (RH) of about 80% [52]. It was found that Pd/Silicalite-1 gradually became inactive after 30 h of operation, but the activity of Pd/TS-1 remained stable after 1900 h of reaction. The extended X-ray absorption fine structure (EXAFS) analysis of the Ti *K*-edge and Pd *K*-edge proved the anchoring effect of Ti on Pd, and the high stability of the porous catalyst was mainly assigned to the hydrophobicity and low acidity of the aluminum-free molecular sieve. Rational use of newly developed techniques could improve the dispersion of PdO and enhance its interaction with the zeolite support.

High-Si zeolites with an MFI framework have recently gained much attention, probably due to the water-related problems and the increasing interest in its hydrophobic property. For example, silicalite-1 (S-1) is an Al-free MFI zeolite and thus lacks acidic sites, but it is highly hydrophobic and hydrothermally stable. Wang et al. claimed that the Pd particles confined in S-1 and the synthesized core-shell catalysts showed high activities at low temperatures, with a shielding impact on H_2O

resistance [53]. Furthermore, due to the hydrophobicity of S-1, Pd@S-1 was able to selectively prevent water vapor from diffusing into the Pd sites, exhibiting outstanding water resistance. In addition, Pd@S-1 and $Pd_{0.8}Ni_{0.2}$@S-1 showed the $T_{90\%}$ of 385 and 412 °C in the presence of 5 vol% water vapor [54], respectively. It is widely accepted in a number of the literature works that the small PdO NPs encapsulated in the zeolitic crystals are the active sites, which can prevent Pd from migrating and sintering and improve the stability of the zeolite-supported PdO catalysts under harsh conditions.

4. Large-Pore Zeolites with 12 Member Rings

In addition to the small and medium pore size zeolites mentioned above, the noble metal catalysts supported on large pore size zeolites (BEA, pore size = 0.7–0.8 nm) for CH_4 combustion applications have also been reported before. For example, Zhang et al. deposited Pd on the dealuminated zeolite support via a reduction—deposition route to generate the high-efficiency Pd/beta catalyst for lean CH_4 combustion [55]. The Pd/beta catalyst at a Pd loading of 0.5 wt% showed excellent catalytic activity (methane conversion > 99% at 375 °C) and good stability. The good performance of Pd/beta was ascribed to the highly dispersed PdO NPs, abundant adsorbed oxygen species, stable PdO, rich Pd^{n+} ($0 < n < 2$) species anchored at the T-atom site, and enhanced hydrophobicity. It is generally recognized that dealumination can reduce the crystallinity of a zeolite and lead to the formation of the aluminum species outside the acidic framework, which further promotes the sintering of palladium particles. Subsequently, they also introduced an organic ligand of 3-mercaptopropyl trimethoxysilane (MPTS) to stabilize the Pd precursor during the preparation process, which was used to confine the PdO NPs in the beta zeolite [56]. The as-obtained sample demonstrated prominent CH_4 combustion activity (99% CH_4 conversion at 360 °C) and exhibited a remarkably better anti-sintering property and long-term (50 h) stability than the Pd/beta-IW and Pd/beta-HT samples. Kröcher et al. designed a porous catalyst based on Pd and a hierarchical zeolite with the fully Na-exchanged acid sites, which improved the support stability and prevents steam-induced Pd sintering under the reaction conditions by confining the noble metal within the zeolite [57]. Under the dry and wet conditions, the $T_{50\%}$ values over Pd/Na-MOR were 340 and 375 °C, respectively. There was no deactivation of this catalyst after 90 h of reaction in the presence of water. Ghorbel et al. prepared the Pd and Pd–Mo catalysts supported on HY and NaY and studied the effect of molybdenum doping on the activity of the catalyst [58]. It was found that Pd/HY and PdMo/NaY were less active than Pd/NaY at 500 °C. The catalytic activity of the monometallic sample increased with the reaction time, whereas that of the bimetallic sample decreased. The comparison of the catalytic activity of Pd/HY or PdMo/NaY revealed that the basicity of the support enhanced the oxidation ability of Pd by a rise in the electronic density of the metal particles on the sample surface.

5. Mesoporous Zeolite and Mesoporous Silicas Catalysts

The pore sizes of the conventional zeolites are generally less than 2 nm, and the reactants can be readily blocked from entering the active centers. The introduction of another set of mesopore nanochannels (so-called mesoporous zeolites) can considerably enhance the mass transfer efficiency, which structurally favors most of the reactions. Mesoporous silica zeolites are one of the most attractive catalytic materials for methane combustion because of their good chemical stability at high temperatures. More importantly, the mesoporous channels of such materials can provide limited space for the formation of Pd NPs with suitable sizes, and control the Pd species in their most active state, which shows the interesting activities of the as-designed catalysts [59].

Hussain et al. prepared the mesoporous silica-supported Pd catalysts and measured their catalytic activities for methane combustion [60]. Benefiting from the suitable structure and pore size of the silica, all the as-obtained Pd catalysts exhibited an almost complete conversion of CH_4, although the catalysts with the lowest Pd loading showed a methane conversion of 90% at 650 °C, whereas the maximum Pd loading in the KIT-6-supported catalyst allowed for a decrease in the temperature ($T_{90\%}$ = 405 °C for complete conversion of methane). Yuranov and coworkers successfully encapsulated Pd NPs with particle sizes of 1.0–3.6 nm within the channels of SBA-15 using the ion exchange strategy [61]. It was found that through the ion exchange of the surface silanol groups with $[Pd(NH_3)_4]^{2+}$, the Pd loadings (0.1–4.4 wt%) could be further increased. The transmission electron microscopic (TEM) investigations of 2.1 wt% Pd/SBA-15-extr. indicated that most of the Pd NPs were located inside the mesoporous channels. The 2.1 wt% Pd/SBA-15 catalyst showed a stable catalytic activity in 6 h on-stream methane combustion at 520 °C.

The above research advances exemplify the feasibility of mesoporous silica (especially SBA-15) as a support for loading Pd and the effectiveness of the ion exchange method in maximizing the reactivity of the Pd species in methane combustion. Murthy et al. used the sol immobilization (SI) method instead of the conventional initial wet impregnation (IWI) method to prepare uniform Pd NPs confined in ordered mesoporous SBA-15 and determined their activities for methane combustion [62]. Compared with the catalyst derived from the conventional IWI method, the one derived from the SI route possessed uniform Pd NPs with a size of 5 nm in the channels of SBA-15 and still maintained such a size even

after thermal aging in air at 800 °C for 3 days. The thermally stable Pd/SBA-15-SI catalyst showed excellent activity for CH_4 combustion ($T_{50\%}$ = 300 °C and $T_{90\%}$ = 350 °C), which was consistent with the result reported in the literature [63]. Afterward, Zribi et al. also synthesized a highly dispersed PdO (particle size = 2 nm) phase in MCM-41, and the Pd(II) complex with a monoamine ligand was used to prevent precipitation of the Pd precursor [64].

The doping of a substance with a redox nature is conducive to the construction of the metal—support interaction, improves stability of the target catalyst, and reduces the use of precious metals [10][19][21]. Liotta et al. prepared the SBA-15-supported $LaMn_{0.4}Fe_{0.6}O_3$ catalysts with perovskite loadings of 10, 30, and 40 wt% and found that the CH_4 combustion activity of the Pd/30 wt% $LaMn_{0.4}Fe_{0.6}O_3$/SBA-15 catalyst was improved compared with that of the Pd/$LaMn_{0.4}Fe_{0.6}O_3$ catalyst [65]. The Pd/30 wt% $LaMn_{0.4}Fe_{0.6}O_3$/SBA-15 catalyst also showed excellent SO_2 tolerance. Based on the structure and spectral characterization results, the optimized catalytic activity was due to the high dispersion of the active sites and good resistance to sintering during the reaction process. Yin et al. used the impregnation method to prepare a series of catalysts with different Pd loadings and investigated their catalytic activities and stability under the lean CH_4 combustion conditions [66]. The introduction of ZrO_2 as a promoter led to the enhancements in the oxygen storage ability and oxygen mobility of the catalyst. Among all the catalysts, 0.5 wt% Pd/5 wt% ZrO_2/SBA-15 exhibited the best catalytic performance and stability. After 400 h of an on-stream reaction at 450 ℃, the methane conversions remained unchanged. Ruiz et al. investigated the catalytic activities of the MCM-41-supported Pd catalysts for methane combustion [67]. Although the change in structure was not observed, the addition of La or Ce gave rise to a decrease in the catalytic activity of the methane combustion, and the all-silicate-based catalyst was more active than the Pd sample supported on aluminosilicate. In addition, the hydrophobic nature of the support and the reducibility of PdO were the main factors influencing the performance of the catalyst.

Peng et al. developed a facile in situ mesoporous-free strategy to synthesize Pd NPs enveloped in a single-crystal S-1 zeolite with intra-mesopores (Pd@IM-S-1) [68]. The Pd@IM-S-1 catalyst exhibited good performance for the deep oxidation of light alkanes (the $T_{90\%}$ was as low as 318 °C for CH_4 combustion), which was attributable to the confinement effect of the zeolite shell and improvement in the mass transfer efficiency and accessibility of the active metal sites. The Pd-PdO interface as a new active site could provide the active oxygen species for cleavage of the first C–H bond in light alkanes. It is proved that the restriction of zeolite channels further protects PdO NPs from sintering or hydrothermal aging under methane oxidation conditions, giving rise to high catalytic activity, stable operation durability, and good high-temperature stability. However, what can confine the active site is still controversial. In short, all kinds of zeolite supports with different skeleton architectures and pore diameters (i.e., micro- and mesopores) are suitable as supports of the Pd-based catalysts for CH_4 combustion.

6. Other Noble Metal-Based Zeolite Catalysts

Rh has been far less studied for CH_4 combustion, but it is an important component in the three-way catalysts, which can improve the catalytic activity and stability of the catalysts. Christensen et al. examined the impacts of temperature and SO_2 concentration (1–20 ppm) on the activity of the catalysts [69]. The deactivation induced by sulfur dioxide introduction was intensified with the drop in temperature or the rise in SO_2 concentration, and such a SO_2 poisoning could be thought to be due to partial or complete occupation of the active sites (which exhibits a Temkin adsorption isotherm). In the presence of 1–2 ppm SO_2, full coverage of the S-containing species was reached at 400 °C, but the coverage was significantly decreased at 500 °C, and significant catalytic activity was retained in the presence of SO_2. Recently, the same group reported that the 2 wt% Rh/ZSM-5 catalyst showed high methane conversions at high space velocities in the presence of water and sulfur dioxide [70]. The Rh-based catalysts with the presence of Rh_2O_3 were superior to the Pd-based catalysts in the presence of H_2O and SO_2. Although both water and sulfur dioxide decreased the activities of the supported Pd and Rh catalysts, water was found to exert a destabilizing effect on rhodium sulfate, i.e., the presence of water caused the sulfate to be partially decomposed below 400 °C, which could partly alleviate the sulfur dioxide poisoning of the supported Rh catalysts. The combined inhibition derived from (H_2O + SO_2) was weaker for the supported Rh catalysts than that for the supported Pd catalysts. In fact, the research works on CH_4 combustion over the supported Rh catalysts are relatively insufficient in the literature. In addition to the aluminosilicate zeolites, the silico-alumino-phosphate (SAPO) molecular sieves were also thought to be promising support materials. Nomura et al. studied CH_4 combustion over the Pd-SAPO-5 catalyst and found that steam strongly inhibited methane combustion [71]. Under the same conditions (10 vol% water vapor), the bimetallic Pd-Pt-SAPO-5 catalyst showed better methane combustion activity after the doping of Pt. Osman et al. investigated that the four-component catalyst containing bimetallic Pt and Pd NPs (for stability), TiO_2 (for oxygen mobility), and η-Al_2O_3 or H-ZSM-5 (acidic support) was superior to the simpler catalysts [72]. The multi-component catalyst with the optimized parameters obviously promoted the enhancement in methane combustion activity ($T_{90\%}$ = 200 °C at a GHSV of 10,000 mL/(gh)), and the long-term fluidization experiment showed that

the activity of the catalyst did not decrease after more than 50 h of reaction at 250 °C. Meanwhile, Dai et al. prepared the PdO/CeO_2 nanosheets wrapped by the HZSM-5 film hybrid composite with sandwich and core-shell structures [73]. The as-synthesized materials exhibited excellent catalytic performance for methane combustion ($T_{90\%}$ = 495 °C, turnover rate (TOR) = 0.618 s^{-1}), and the HZSM-5 coating improved the resistance to sintering, oxygen, and water, while severe sintering of the conventionally prepared PdO/CeO_2 catalyst was suffered at high temperatures or oxygen concentrations. These results demonstrate that the multi-component catalysts possess better stability than the single Pd catalysts, and the doping of a suitable metal may stabilize the activity of the Pd-based catalyst. In practice, the design of a multi-component catalyst is beneficial for the enhancement of the low-temperature combustion of methane.

So far, the topological structure of a zeolite does not play the most important role in governing the activity of the zeolite-based catalyst for CH_4 combustion. Researchers are more inclined to control the molecular sieve in a beneficial way so as to obtain a high and stable methane oxidation catalyst with better performance.

References

1. Ai, X.Y.; Hu, C.; Yang, Y.R.; Zhang, L.Y.; Liu, H.L.; Zhang, J.Q.; Chen, X.; Bai, G.Q.; Xiao, W. Quantification of Central and Eastern China's atmospheric CH4 enhancement changes and its contributions based on machine learning approach. J. Environ. Sci. 2023, 138, 236–248.
2. Francoeur, C.B.; McDonald, B.C.; Gilman, J.B.; Zarzana, K.J.; Dix, B.; Brown, S.S.; de Gouw, J.A.; Frost, G.J.; Li, M.; McKeen, S.A.; et al. Quantifying methane and ozone precursor emissions from oil and gas production regions across the contiguous US. Environ. Sci. Technol. 2021, 55, 9129–9139.
3. Feng, X.B.; Jiang, L.; Li, D.Y.; Tian, S.P.; Zhu, X.; Wang, H.; He, C.; Li, K.Z. Progress and key challenges in catalytic combustion of lean methane. J. Energy Chem. 2022, 75, 173–215.
4. Zhang, Y.Z.; Fang, S.X.; Chen, J.M.; Lin, Y.; Chen, Y.Y.; Liang, R.S.; Jiang, K.; Parker, R.J.; Boesch, H.; Steinbacher, M.; et al. Observed changes in China's methane emissions linked to policy drivers. Proc. Natl. Acad. Sci. USA 2022, 119, e2202742119.
5. He, L.; Fan, Y.L.; Bellettre, J.; Yue, J.; Luo, L.G. A review on catalytic methane combustion at low temperatures: Catalysts, mechanisms, reaction conditions and reactor designs. Renew. Sustain. Energy Rev. 2020, 119, 109589.
6. Farrauto, R.J. Low-temperature oxidation of methane. Science 2012, 337, 659–660.
7. Chen, J.H.; Arandiyan, H.; Gao, X.; Li, J.H. Recent advances in catalysts for methane combustion. Catal. Surv. Asia 2015, 19, 140–171.
8. Chen, J.J.; Zhong, J.W.; Wu, Y.; Hu, W.; Qu, P.F.; Xiao, X.; Zhang, G.C.; Liu, X.; Jiao, Y.; Zhong, L.; et al. Particle size effects in stoichiometric methane combustion: Structure-activity relationship of Pd catalyst supported on gamma-alumina. ACS Catal. 2020, 10, 10339–10349.
9. Wang, Y.; Arandiyan, H.; Scott, J.; Akia, M.; Dai, H.X.; Deng, J.G.; Aguey-Zinsou, K.; Amal, R. High performance Au–Pd supported on 3D hybrid strontium-substituted lanthanum manganite perovskite catalyst for methane combustion. ACS Catal. 2016, 6, 6935–6947.
10. Xiong, H.F.; Kunwar, D.; Jiang, D.; García-Vargas, C.E.; Li, H.; Du, C.; Canning, G.; Pereira-Hernandez, X.I.; Wan, Q.; Lin, S.; et al. Engineering catalyst supports to stabilize PdOx two-dimensional rafts for water-tolerant methane oxidation. Nat. Catal. 2021, 4, 830–839.
11. Xu, P.; Zhang, X.; Zhao, X.T.; Yang, J.; Hou, Z.Q.; Bai, L.; Chang, H.Q.; Liu, Y.X.; Deng, J.G.; Guo, G.S.; et al. Preparation, characterization, and catalytic performance of PdPt/3DOM LaMnAl11O19 for the combustion of methane. Appl. Catal. A 2018, 562, 284–293.
12. Yang, J.; Hu, S.Y.; Shi, L.M.; Hoang, S.; Yang, W.W.; Fang, Y.R.; Liang, Z.F.; Pan, C.Q.; Zhu, Y.H.; Li, L.; et al. Oxygen vacancies and Lewis acid sites synergistically promoted catalytic methane combustion over perovskite oxides. Environ. Sci. Technol. 2021, 55, 9243–9254.
13. Zhao, X.T.; Zhang, R.; Liu, Y.X.; Deng, J.G.; Xu, P.; Yang, J.; Han, Z.; Hou, Z.Q.; Dai, H.X.; Au, C.T. In-situ reduction-derived Pd/3DOM La0.6Sr0.4MnO3: Good catalytic stability in methane combustion. Appl. Catal. A 2018, 568, 202–212.
14. Gélin, P.; Primet, M. Complete oxidation of methane at low temperature over noble metal based catalysts: A review. Appl. Catal. B 2002, 39, 1–37.
15. Park, J.; Ahn, J.; Sim, H.; Seo, G.; Han, H.S.; Shin, C. Low-temperature combustion of methane using PdO/Al2O3 catalyst: Influence of crystalline phase of Al2O3 support. Catal. Commun. 2014, 56, 157–163.

16. Beck, I.E.; Bukhtiyarov, V.I.; Pakharukov, I.Y.; Zaikovsky, V.I.; Kriventsov, V.V.; Parmon, V.N. Platinum nanoparticles on Al2O3: Correlation between the particle size and activity in total methane oxidation. J. Catal. 2009, 268, 60–67.
17. Shi, W.; Xu, G.Y.; Han, X.W.; Wang, Y.J.; Liu, Z.; Xue, S.; Sun, N.N.; Shi, X.Y.; Yu, Y.B.; He, H. Nano-sized alumina supported palladium catalysts for methane combustion with excellent thermal stability. J. Environ. Sci. 2023, 126, 333–347.
18. Hou, Z.Q.; Dai, L.Y.; Deng, J.G.; Zhao, G.F.; Jing, L.; Wang, Y.; Yu, X.H.; Gao, R.Y.; Tian, X.R.; Dai, H.X.; et al. Electronically engineering water resistance in methane combustion with an atomically dispersed tungsten on PdO catalyst. Angew. Chem. Int. Ed. 2022, 61, e202201655.
19. Hou, Z.Q.; Liu, Y.X.; Deng, J.G.; Lu, Y.; Xie, S.H.; Fang, X.; Dai, H.X. Highly active and stable Pd–GaOx/Al2O3 catalysts derived from intermetallic Pd5Ga3 nanocrystals for methane combustion. ChemCatChem 2018, 10, 5637–5648.
20. Liu, Z.; Xu, G.Y.; Zeng, L.Y.; Shi, W.; Wang, Y.J.; Sun, Y.W.; Yu, Y.B.; He, H. Anchoring Pt-doped PdO nanoparticles on γ-Al2O3 with highly dispersed La sites to create a methane oxidation catalyst. Appl. Catal. B 2023, 324, 122259.
21. Ma, X.Y.; Xu, H.; Liu, Z.; Liu, Y.F.; Wang, C.; Shen, M.Q.; Du, C.; Shan, B. Durable PdNi/Al2O3 catalysts with PdO–NiO and PdO–NiAl2O4 dual interfaces for methane combustion. ACS ES&T Eng. 2023, 3, 349–359.
22. Poznyak, A.A.; Knörnschild, G.H.; Pligovka, A.N.; Larin, T.D. Anodic alumina prepared in aqueous solutions of chelating complex zinc and cobalt compounds. Tech. Phys. 2022, 67, 411–422.
23. Poznyak, A.; Knörnschild, G.; Karoza, A.; Norek, M.; Pligovka, A. Peculiar porous aluminum oxide films produced via electrochemical anodizing in malonic acid solution with arsenazo-I additive. Materials 2021, 14, 5118.
24. Chen, S.Y.; Li, S.D.; You, R.Y.; Guo, Z.Y.; Wang, F.; Li, G.X.; Yuan, W.T.; Zhu, B.; Gao, Y.; Zhang, Z.; et al. Elucidation of active sites for CH4 catalytic oxidation over Pd/CeO2 via tailoring metal-support interactions. ACS Catal. 2021, 11, 5666–5677.
25. Colussi, S.; Gayen, A.; Farnesi Camellone, M.; Boaro, M.; Llorca, J.; Fabris, S.; Trovarelli, A. Nanofaceted Pd-O sites in Pd-Ce surface superstructures: Enhanced activity in catalytic combustion of methane. Angew. Chem. Int. Ed. 2009, 48, 8481–8484.
26. Xie, S.H.; Liu, Y.X.; Deng, J.G.; Zhao, X.; Yang, J.; Zhang, K.F.; Han, Z.; Dai, H.X. Three-dimensionally ordered macroporous CeO2-supported Pd@Co nanoparticles: Highly active catalysts for methane oxidation. J. Catal. 2016, 342, 17–26.
27. Yang, W.W.; Polo-Garzon, F.; Zhou, H.; Huang, Z.N.; Chi, M.F.; Meyer, H., III; Yu, X.B.; Li, Y.Y.; Wu, Z.L. Boosting the activity of Pd single atoms by tuning their local environment on ceria for methane combustion. Angew. Chem. Int. Ed. 2023, 62, e202217323.
28. Ding, Y.Q.; Jia, Y.Y.; Jiang, M.X.; Guo, Y.; Guo, Y.; Wang, L.; Ke, Q.P.; Ngoc Ha, M.; Dai, S.; Zhan, W.C. Superior catalytic activity of Pd-based catalysts upon tuning the structure of the ceria-zirconia support for methane combustion. Chem. Eng. J. 2021, 416, 129150.
29. Ding, Y.Q.; Wu, Q.Q.; Lin, B.; Guo, Y.L.; Guo, Y.; Wang, Y.S.; Wang, L.; Zhan, W.C. Superior catalytic activity of a Pd catalyst in methane combustion by fine-tuning the phase of ceria-zirconia support. Appl. Catal. B 2020, 266, 118631.
30. 2Yang, W.W.; Kim, M.Y.; Polo-Garzon, F.; Gong, J.; Jiang, X.; Huang, Z.N.; Chi, M.F.; Yu, X.B.; Wang, X.; Guo, Y.B.; et al. CH4 combustion over a commercial Pd/CeO2–ZrO2 three-way catalyst: Impact of thermal aging and sulfur exposure. Chem. Eng. J. 2023, 451, 138930.
31. Huang, J.L.; Lin, J.; Chen, X.H.; Zheng, Y.; Xiao, Y.H.; Zheng, Y. Optimizing the microstructure of SnO2–CeO2 binary oxide supported palladium catalysts for efficient and stable methane combustion. ACS Appl. Mater. Interfaces 2022, 14, 16233–16244.
32. Takeguchi, T.; Takeoh, O.; Aoyama, S.; Ueda, J.; Kikuchi, R.; Eguchi, K. Strong chemical interaction between PdO and SnO2 and the influence on catalytic combustion of methane. Appl. Catal. A 2003, 252, 205–214.
33. Wang, Y.; Liu, C.W.; Liao, X.M.; Liu, Y.M.; Hou, J.D.; Pham-Huu, C. Enhancing oxygen activation on high surface area Pd–SnO2 solid solution with isolated metal site catalysts for catalytic CH4 combustion. Appl. Surf. Sci. 2021, 564, 150368.
34. Zhao, Z.Y.; Wang, B.W.; Ma, J.; Zhan, W.C.; Wang, L.; Guo, Y.L.; Guo, Y.; Lu, G.Z. Catalytic combustion of methane over Pd/SnO2 catalysts. Chin. J. Catal. 2017, 38, 1322–1329.
35. Willis, J.J.; Gallo, A.; Sokaras, D.; Aljama, H.; Nowak, S.H.; Goodman, E.D.; Wu, L.; Tassone, C.J.; Jaramillo, T.F.; Abild-Pedersen, F.; et al. Systematic structure-property relationship studies in palladium-catalyzed methane complete combustion. ACS Catal. 2017, 7, 7810–7821.

36. Garbowski, E.; Feumi-Jantou, C.; Mouaddib, N.; Primet, M. Catalytic combustion of methane over palladium supported on alumina catalysts: Evidence for reconstruction of particles. Appl. Catal. A 1994, 109, 277–291.

37. Wang, Y.L.; Hu, P.; Yang, J.; Zhu, Y.A.; Chen, D. C–H bond activation in light alkanes: A theoretical perspective. Chem. Soc. Rev. 2021, 50, 4299–4358.

38. Murata, K.; Mahara, Y.; Ohyama, J.; Yamamoto, Y.; Arai, S.; Satsuma, A. The metal–support -interaction concerning the particle size effect of Pd/Al2O3 on methane combustion. Angew. Chem. Int. Ed. 2017, 56, 15993–15997.

39. Hong, E.; Kim, C.; Lim, D.; Cho, H.; Shin, C. Catalytic methane combustion over Pd/ZrO2 catalysts: Effects of crystalline structure and textural properties. Appl. Catal. B 2018, 232, 544–552.

40. Schwartz, W.R.; Ciuparu, D.; Pfefferle, L.D. Combustion of methane over palladium-based catalysts: Catalytic deactivation and role of the support. J. Phys. Chem. C 2012, 116, 8587–8593.

41. Smit, B. Molecular simulations of zeolites: Adsorption, diffusion, and shape selectivity. Chem. Rev. 2008, 108, 4125–4184.

42. Zhao, D.Y.; Feng, J.L.; Huo, Q.S.; Melosh, N.; Fredrickson, G.H.; Chmelka, B.F.; Stucky, G.D. Triblock copolymer syntheses of mesoporous silica with periodic 50 to 300 angstrom pores. Science 1998, 279, 548–552.

43. Kresge, A.C.; Leonowicz, M.E.; Roth, W.J.; Vartuli, J.C.; Beck, J.S. Ordered mesoporous molecular sieves synthesized by a liquid-crystal template mechanism. Nature 1992, 359, 710–712.

44. Kleitz, F.; Hei Choi, S.; Ryoo, R. Cubic Ia3d large mesoporous silica: Synthesis and replication to platinum nanowires, carbon nanorods and carbon nanotubes. Chem. Commun. 2003, 2136–2137.

45. Cui, Y.R.; Chen, J.Z.; Peng, B.; Kovarik, L.; Devaraj, A.; Li, Z.; Ma, T.; Wang, Y.L.; Szanyi, J.; Miller, J.T.; et al. Onset of high methane combustion rates over supported palladium catalysts: From isolated Pd cations to PdO nanoparticles. JACS Au 2021, 1, 396–408.

46. Friberg, I.; Clark, A.H.; Ho, P.H.; Sadokhina, N.; Smales, G.J.; Woo, J.; Auvray, X.; Ferri, D.; Nachtegaal, M.; Kröcher, O.; et al. Structure and performance of zeolite supported Pd for complete methane oxidation. Catal. Today 2021, 382, 3–12.

47. Leistner, K.; Kumar, A.; Kamasamudram, K.; Olsson, L. Mechanistic study of hydrothermally aged Cu/SSZ-13 catalysts for ammonia-SCR. Catal. Today 2018, 307, 55–64.

48. Friberg, I.; Wang, A.; Olsson, L. Hydrothermal aging of Pd/LTA monolithic catalyst for complete CH4 oxidation. Catalysts 2020, 10, 517.

49. Argauer, R.J.; Landolt, G.R. Crystalline Zeolite ZSM-5 and Method of Preparing the Same. U.S. Patent 3702886DA, 14 November 1972.

50. Li, Y.; Armor, J.N. Catalytic combustion of methane over palladium exchanged zeolites. Appl. Catal. B 1994, 3, 275–282.

51. Liu, C.; Yu, K.; Zhang, Y.; Zhu, X.; He, F.; Eliasson, B. Remarkable improvement in the activity and stability of Pd/HZSM-5 catalyst for methane combustion. Catal. Commun. 2003, 4, 303–307.

52. Hosseiniamoli, H.; Setiawan, A.; Adesina, A.A.; Kennedy, E.M.; Stockenhuber, M. The stability of Pd/TS-1 and Pd/silicalite-1 for catalytic oxidation of methane-understanding the role of titanium. Catal. Sci. Technol. 2020, 10, 1193–1204.

53. Wang, W.Y.; Zhou, W.; Li, W.; Xiong, X.W.; Wang, Y.H.; Cheng, K.J.; Kang, J.; Zhang, Q.H.; Wang, Y. In-situ confinement of ultrasmall palladium nanoparticles in silicalite-1 for methane combustion with excellent activity and hydrothermal stability. Appl. Catal. B 2020, 276, 119142.

54. Zhang, Z.S.; Sun, L.W.; Hu, X.F.; Zhang, Y.B.; Tian, H.Y.; Yang, X.G. Anti-sintering Pd@silicalite-1 for methane combustion: Effects of the moisture and SO2. Appl. Surf. Sci. 2019, 494, 1044–1054.

55. Zhang, L.L.; Chen, J.F.; Guo, X.M.; Yin, S.M.; Zhang, M.; Rui, Z.B. Combination of reduction-deposition Pd loading and zeolite dealumination as an effective route for promoting methane combustion over Pd/Beta. Catal. Today 2021, 376, 119–125.

56. Zhang, L.L.; Chen, J.F.; Yang, H.; Wang, X.; Rui, Z.B. In situ mercaptosilane-assisted confinement of Pd nanoparticles in Beta for high-efficient methane oxidation. Catal. Today 2022, 400, 124–131.

57. Petrov, A.W.; Ferri, D.; Krumeich, F.; Nachtegaal, M.; van Bokhoven, J.A.; Kröcher, O. Stable complete methane oxidation over palladium based zeolite catalysts. Nat. Commun. 2018, 9, 2545.

58. Zina, M.S.; Ghorbel, A. Preparation and characterization of bimetallic PdMo/Y-zeolite: Catalytic properties in methane combustion. Solid State Sci. 2004, 6, 973–980.

59. Song, H.; Rioux, R.M.; Hoefelmeyer, J.D.; Komor, R.; Niesz, K.; Grass, M.; Yang, P.; Somorjai, G.A. Hydrothermal growth of mesoporous SBA-15 silica in the presence of PVP-stabilized Pt nanoparticles: Synthesis, characterization, and catalytic properties. J. Am. Chem. Soc. 2006, 128, 3027–3037.
60. Hussain, M.; Deorsola, F.A.; Russo, N.; Fino, D.; Pirone, R. Abatement of CH4 emitted by CNG vehicles using Pd-SBA-15 and Pd-KIT-6 catalysts. Fuel 2015, 149, 2–7.
61. Yuranov, I.; Moeckli, P.; Suvorova, E.; Buffat, P.; Kiwi-Minsker, L.; Renken, A. Pd/SiO2 catalysts: Synthesis of Pd nanoparticles with the controlled size in mesoporous silicas. J. Mol. Catal. A 2003, 192, 239–251.
62. Murthy, P.R.; Zhang, J.; Li, W. Exceptionally stable sol-immobilization derived Pd/SBA-15 catalysts for methane combustion. Catal. Sci. Technol. 2021, 11, 3609–3618.
63. Li, C.S.; Tang, B.Y.; Li, W.Z.; Lu, Q.; Yuan, L. Palladium nanoparticles encapsulated in surface-defected SBA-15 for lean methane oxidation. ACS Appl. Nano Mater. 2022, 5, 13055–13068.
64. Zribi, S.; Albela, B.; Bonneviot, L.; Zina, M.S. Surface engineering and palladium dispersion in MCM-41 for methane oxidation. Appl. Catal. A 2015, 502, 195–203.
65. Liotta, L.F.; Di Carlo, G.; Pantaleo, G.; Hernandez Garrido, J.C.; Venezia, A.M. Pd (1 wt%)/LaMn0.4Fe0.6O3 catalysts supported over silica SBA-15: Effect of perovskite loading and support morphology on methane oxidation activity and SO2 tolerance. Top. Catal. 2012, 55, 782–791.
66. Yin, F.X.; Ji, S.F.; Wu, P.Y.; Zhao, F.Z.; Li, C.Y. Deactivation behavior of Pd-based SBA-15 mesoporous silica catalysts for the catalytic combustion of methane. J. Catal. 2008, 257, 108–116.
67. Ruiz, J.A.; Fraga, M.A.; Pastore, H.O. Methane combustion over Pd supported on MCM-41. Appl. Catal. B 2007, 76, 115–122.
68. Peng, H.G.; Dong, T.; Yang, S.; Chen, H.; Yang, Z.Z.; Liu, W.M.; He, C.; Wu, P.; Tian, J.; Peng, Y.; et al. Intra-crystalline mesoporous zeolite encapsulation-derived thermally robust metal nanocatalyst in deep oxidation of light alkanes. Nat. Commun. 2022, 13, 295.
69. Zhang, Y.; Glarborg, P.; Andersson, M.P.; Johansen, K.; Torp, T.K.; Jensen, A.D.; Christensen, J.M. Sulfur poisoning and regeneration of Rh-ZSM-5 catalysts for total oxidation of methane. Appl. Catal. B 2020, 277, 119176.
70. Zhang, Y.; Glarborg, P.; Johansen, K.; Andersson, M.P.; Torp, T.K.; Jensen, A.D.; Christensen, J.M. A rhodium-based methane oxidation catalyst with high tolerance to H2O and SO2. ACS Catal. 2020, 10, 1821–1827.
71. Nomura, K.; Noro, K.; Nakamura, Y.; Yazawa, Y.; Yoshida, H.; Satsuma, A.; Hattori, T. Pd-Pt bimetallic catalyst supported on SAPO-5 for catalytic combustion of diluted methane in the presence of water vapor. Catal. Lett. 1998, 53, 167–169.
72. Osman, A.I.; Abu-Dahrieh, J.K.; Laffir, F.; Curtin, T.; Thompson, J.M.; Rooney, D.W. A bimetallic catalyst on a dual component support for low temperature total methane oxidation. Appl. Catal. B 2016, 187, 408–418.
73. Dai, Q.G.; Bai, S.; Lou, Y.; Wang, X.; Guo, Y.; Lu, G.Z. Sandwich-like PdO/CeO2 nanosheet@HZSM-5 membrane hybrid composite for methane combustion: Self-redispersion, sintering-resistance and oxygen, water-tolerance. Nanoscale 2016, 8, 9621–9628.